11th International Conference on Vibration Problems
Z. Dimitrovová *et al.* (eds.)
Lisbon, Portugal, 9-12 September 2013

DYNAMIC RESPONSE CONTROL OF AN ELECTRORHEOLOGICAL FLUID-BASED ADAPTIVE PLATE RESTING ON ELASTIC FOUNDATION

M. E. Aryaee Panah[*1], Seyyed M. Hasheminejad[2], and M. Nezami[3]

[1]University of Southern Denmark, Sønderborg, Denmark
mopan11@student.sdu.dk

[2]Acoustics Research Laboratory, School of Mechanical Engineering,Iran University of Science and Technology, Tehran, Iran; hashemi@iust.ac.ir

[3]Department of mechanical engineering, Firoozkooh branch,islamic azad university,Firoozkooh,Iran

Abstract: *The field-dependent dynamic response of a simply supported rectangular orthotropic sandwich plate containing a tunable electro-rheological fluid (ERF) interlayer, while resting on a Winkler-Pasternak foundation and subjected to general arbitrary transient transverse loading, is studied. The ER fluid core is modeled as a first order Kelvin-Voigt material and Hamilton's principle along with the classical plate theory are used to derive a set of fully coupled dynamic equations of motion. The generalized Fourier series in conjunction with Durbin's numerical Laplace inversion scheme are subsequently employed to calculate the displacement response for selected applied electric field strengths (E=0, 5kV/mm), with or without a soft/stiff elastic foundation, in various basic loading configurations (i.e., impulsive or moving point loads, and uniformly distributed harmonic, load). The governing equations of motion are put in a state space form and a sliding mode control (SMC) strategy coupled with the classical Runge-Kutta time integration algorithm, are applied to actively control the response of the system to the imposed excitations. Simulation results demonstrate that the SMC-based control system can attenuate plate vibrations effectively and exhibits excellent performance robustness with respect to the control spillover and the different types of disturbances considered. Limiting cases are considered and good agreements with the data available in the literature as well as with the computations made by using the Rayleigh-Ritz approach are obtained.*

1 INTRODUCTION

Beams, plates, and panels are commonly used as flexible structural components in various areas of modern engineering disciplines. These structures are often subjected to complicated external dynamic excitations such as nuclear blast, sonic boom, shock waves, moving loads, earthquakes, impacts, and other conditions, which can make them unstable. Various methods to suppress such vibrations have been proposed which commonly comprise passive, active, semi-active and hybrid vibration control systems [1]. In particular, intelligent materials such as piezoelectric materials [2], shape memory alloys [3], electro-strictive materials [4], and electro- or magneto-rheological fluids [5] are commonly incorporated as distributed actuators into conventional structures to actively control vibrations and improve performance. Adaptive structures utilizing tunable electro- or magneto-rheological fluids (ERFs or MRFs) have the beneficial control capabilities of rapidly and reversibly changing the damping and stiffness characteristics of the system by application of an external electric/magnetic field, in addition to the other valuable features of low-energy loss, reliability and easy controllability by computers [6]. Various control strategies have been employed for controller design of ER-based devices and structures. For example, the sliding mode theory ([7], [8]), Lyapunov stability theory ([9], [10]), neural network [11], linear proportional feedback [12], nonlinear compensation technique [13], and fuzzy-like logic controller [14], to name a few, have been employed.

The above short review clearly indicates that while there exists a notable body of literature investigating the free or steady-state vibrational characteristics of electro-rheological fluid-based sandwich plate structures [5], [15], rigorous analytical or numerical solutions describing the dynamic time-domain response of such structures seems to be absent. More importantly, there appears to be no research works in the current literature dealing with closed-loop vibration control of ERF- or MRF-based adaptive plates under arbitrary dynamic loading conditions. The primary purpose of the current work is to fill these important gaps in the literature.

2 FORMULATION

2.1 BASIC RELATIONS

The complete configuration of the sandwich rectangular plate $(a \times b)$ consisting of a base plate (thickness h_3), a constraining layer (thickness h_1), and a tunable fluid core layer (thickness h_2), all resting on a two parameter Winkler-Pasternak foundation with elastic parameters (K_f, G_f), is illustrated in Fig. 1. The base and constraining layers are assumed to be cross-ply elastic composite laminates, with no slipping relative to the core layer. The transverse displacements, w, of every point on a cross-section of the sandwich plate are assumed to be the same. Also, the normal and inplane shear stresses in the core layer as well as the transverse shear strains in the laminated layers 1 and 3 are assumed to be absent. Thus, assuming linear strain-displacement relations, the strain components in the elastic cross-ply laminated layers (layers 1,3) along with the transverse shear strain components in the core fluid (layer 2), are written as [5]

$$\varepsilon_x^{(i)} = \frac{\partial u_i}{\partial x} - z_i \frac{\partial^2 w}{\partial x^2}, \qquad \gamma_{xz}^{(2)} = \frac{l_x}{h_2} = \frac{d}{h_2}\frac{\partial w}{\partial x} + \frac{(u_1 - u_3)}{h_2},$$

$$\varepsilon_y^{(i)} = \frac{\partial v_i}{\partial y} - z_i \frac{\partial^2 w}{\partial y^2}, \qquad \gamma_{yz}^{(2)} = \frac{l_y}{h_2} = \frac{d}{h_2}\frac{\partial w}{\partial y} + \frac{(v_1 - v_3)}{h_2}, \qquad (1)$$

$$\gamma_{xy}^{(i)} = \frac{\partial u_i}{\partial y} + \frac{\partial v_i}{\partial x} - 2z_i \frac{\partial^2 w}{\partial x \partial y},$$
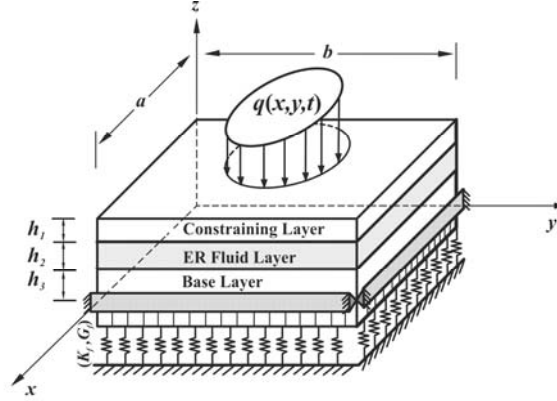

Figure 1: Problem geometry

where z_i ($i = 1,3$) is the transverse coordinate in the local coordinate system of the upper and lower layers positioned at their associated mid-planes, $l_x = d\theta_x + (u_1 - u_3)$ and $l_y = d\theta_y + (v_1 - v_3)$; $d = h_1/2 + h_2 + h_3/2$, and $u_i(x,y)$ and $v_i(x,y)$ which respectively are the mid-plane deformations in the x and y directions, are related to the total displacement components at a material point (x,y,z) within the upper and lower elastic laminates through the kinematical relations [16]:

$$u^{(i)}(x,y,z,t) = u_i(x,y,t) - z_i \frac{\partial w(x,y,t)}{\partial x},$$
$$v^{(i)}(x,y,z,t) = v_i(x,y,t) - z_i \frac{\partial w(x,y,t)}{\partial y}, \qquad (2)$$
$$w^{(i)}(x,y,z,t) = w(x,y,t),$$

where $i = 1,3$. In addition, assuming a state of plane stress within the upper and lower cross-ply laminates entails that the stress components within the k-th orthotropic lamina in each elastic layer can be obtained from Hooke's law as [16]:

$$\begin{bmatrix} \sigma_x^{(i)} \\ \sigma_y^{(i)} \\ \sigma_{xy}^{(i)} \end{bmatrix}^{(k)} = \begin{bmatrix} \bar{Q}_{11}^{(i)} & \bar{Q}_{12}^{(i)} & 0 \\ \bar{Q}_{12}^{(i)} & \bar{Q}_{22}^{(i)} & 0 \\ 0 & 0 & \bar{Q}_{66}^{(i)} \end{bmatrix}^{(k)} \begin{bmatrix} \varepsilon_x^{(i)} \\ \varepsilon_y^{(i)} \\ \gamma_{xy}^{(i)} \end{bmatrix}^{(k)}, \qquad (3)$$

where $\bar{Q}_{\alpha\beta}^{(i)}$ ($i=1,3$) are the stiffness constants in each orthotropic lamina within the i-th layer ($i=1,3$) which in the case of isotropic materials reduce to

$$\bar{Q}_{11}^{(i)} = \bar{Q}_{22}^{(i)} = \frac{E_i}{1 - \nu_i^2}, \quad \bar{Q}_{12}^{(i)} = \frac{\nu_i E_i}{1 - \nu_i^2}, \quad \bar{Q}_{66}^{(i)} = \frac{E_i}{2(1 + \nu_i)},$$

where E_i and ν_i are the corresponding Young modulus and Poisson ratio, respectively. Here we shall model the ER fluid core by a first order isotropic Kelvin-Voigt viscoelastic material in the pre-yield regime, whose pertinent constitutive equations in the time domain are written as [17]:

$$\sigma_{xz}^{(2)} = G_2 \gamma_{xz}^{(2)} + \eta_2 \dot{\gamma}_{xz}^{(2)},$$
$$\sigma_{yz}^{(2)} = G_2 \gamma_{yz}^{(2)} + \eta_2 \dot{\gamma}_{yz}^{(2)}, \qquad (4)$$

where $\eta_2(t) = m_e E(t) + b_e$ and $G_2(t) = m_g E(t) + b_g$ denote the electric field-dependent viscosity and elasticity of the electrorheological core fluid layer, respectively, and $E(t)$ is the time-dependant electric field (kV/mm).

2.2 EQUATIONS OF MOTION AND BOUNDARY CONDITIONS

In this subsection, Hamilton's variational principle is employed to derive the governing equations of motion for the sandwich rectangular plate in the time domain along with the associated general boundary conditions, based on the classical thin plate theory. Following the standard procedure, one should extremize the time integral of the Lagrangian for the entire system in any arbitrarily time interval, i.e.,

$$\delta I = \delta \int_{t_1}^{t_2} L dt = \delta \int_{t_1}^{t_2} (T - U + W) dt = 0, \tag{5}$$

where δ denotes the first variation operator, W represents the work done by the nonconservative forces, L is the Lagrangian function, T is the kinetic energy, and $U = U_p + U_f$ is total strain energy of the plate-foundation system. Also, the variations of the total work done by the external transverse distributed force, $q(x,y,t)$, and the damping force, the total kinetic energy of the sandwich plate, and the strain energies of the sandwich plate and the elastic foundation, can respectively be written as:

$$\delta W = \int_\Omega q \delta w \, d\Omega - \eta_2 h_2 \int_\Omega \left(\dot{\gamma}_{xz}^{(2)} \delta \gamma_{xz}^{(2)} + \dot{\gamma}_{yz}^{(2)} \delta \gamma_{yz}^{(2)} \right) d\Omega,$$

$$\delta T = \sum_{i=1,3} \delta \int_\Omega \frac{1}{2} \rho_i h_i (\dot{u}_i^2 + \dot{v}_i^2 + \dot{w}^2) d\Omega + \delta \int_\Omega \frac{1}{2} \left(\rho_2 h_2 \dot{w}^2 + I_2 \left[(\dot{\gamma}_{xz}^{(2)})^2 + (\dot{\gamma}_{yz}^{(2)})^2 \right] \right) d\Omega,$$

$$\delta U_p = \sum_{i=1,3} \int_{V_i} \left(\sigma_x^{(i)} \delta \varepsilon_x^{(i)} + \sigma_y^{(i)} \delta \varepsilon_y^{(i)} + \sigma_{xy}^{(i)} \delta \gamma_{xy}^{(i)} \right) dV_i + \int_{V_2} \left(G_2 \gamma_{xz}^{(2)} \delta \gamma_{xz}^{(2)} + G_2 \gamma_{yz}^{(2)} \delta \gamma_{yz}^{(2)} \right) dV_2,$$

$$\delta U_f = \int_\Omega (K_f w - G_f \nabla^2 w) \delta w \, d\Omega,$$

$$\tag{6}$$

where $V_i (i = 1,2,3)$ denote the three dimensional domains for the upper, core, and bottom layers, respectively, Ω signifies the two dimensional $(a \times b)$ surface of each layer in the x-y plane, $\rho_i (i = 1,2,3)$ denotes the mass density in the i-th layer, and $I_2 (= \rho_2 h_2^3 / 12)$ is the mass moment of inertia of the core layer. Next, employing expressions (1), (3), (4) in (6), and subsequent substitution in the Lagrangian function, $L = T - U + W$, yields

$$-\sum_{i=1,3} \left\{ \int_\Omega \left[\left(A_{11}^{(i)} \frac{\partial u_i}{\partial x} + A_{12}^{(i)} \frac{\partial v_i}{\partial y} - B_{11}^{(i)} \frac{\partial^2 w}{\partial x^2} - B_{12}^{(i)} \frac{\partial^2 w}{\partial y^2} \right) \frac{\partial \delta u_i}{\partial x} - \left(B_{11}^{(i)} \frac{\partial u_i}{\partial x} + B_{12}^{(i)} \frac{\partial v_i}{\partial y} - D_{11}^{(i)} \frac{\partial^2 w}{\partial x^2} - D_{12}^{(i)} \frac{\partial^2 w}{\partial y^2} \right) \frac{\partial^2 \delta w}{\partial x^2} \right. \right.$$

$$+ \left(A_{12}^{(i)} \frac{\partial u_i}{\partial x} + A_{22}^{(i)} \frac{\partial v_i}{\partial y} - B_{12}^{(i)} \frac{\partial^2 w}{\partial x^2} - B_{22}^{(i)} \frac{\partial^2 w}{\partial y^2} \right) \frac{\partial \delta v_i}{\partial y} + \left(D_{12}^{(i)} \frac{\partial^2 w}{\partial x^2} + D_{22}^{(i)} \frac{\partial^2 w}{\partial y^2} - B_{12}^{(i)} \frac{\partial u_i}{\partial x} - B_{22}^{(i)} \frac{\partial v_i}{\partial y} \right) \frac{\partial^2 \delta w}{\partial y^2}$$

$$+ \left(A_{66}^{(i)} \left(\frac{\partial u_i}{\partial y} + \frac{\partial v_i}{\partial x} \right) - 2 B_{66}^{(i)} \frac{\partial^2 w}{\partial x \partial y} \right) \left(\frac{\partial \delta u_i}{\partial y} + \frac{\partial \delta v_i}{\partial x} \right) - 2 \left(B_{66}^{(i)} \left(\frac{\partial u_i}{\partial y} + \frac{\partial v_i}{\partial x} \right) - 2 D_{66}^{(i)} \frac{\partial^2 w}{\partial x \partial y} \right) \frac{\partial^2 \delta w}{\partial x \partial y} \right] d\Omega \right\}$$

$$-\int_\Omega G_2\left[\left(d\frac{\partial w}{\partial x}+u_1-u_3\right)\left(\frac{d}{h_2}\frac{\partial\delta w}{\partial x}+\frac{\delta u_1-\delta u_3}{h_2}\right)+\left(d\frac{\partial w}{\partial y}+v_1-v_3\right)\left(\frac{d}{h_2}\frac{\partial\delta w}{\partial y}+\frac{\delta v_1-\delta v_3}{h_2}\right)\right]d\Omega$$

$$-\int_\Omega\left[K_fw-G_f\left(\frac{\partial^2 w}{\partial x^2}+\frac{\partial^2 w}{\partial y^2}\right)\right]\delta w d\Omega-\sum_{i=1,3}\int_\Omega\rho_ih_i(\ddot{u}_i\delta u_i+\ddot{v}_i\delta v_i+\ddot{w}\delta w)d\Omega$$

$$-\int_\Omega\left[\rho_2h_2\ddot{w}\delta w+I_2\left(\frac{d}{h_2}\frac{\partial\ddot{w}}{\partial x}+\frac{\ddot{u}_1-\ddot{u}_3}{h_2}\right)\left(\frac{d}{h_2}\frac{\partial\delta w}{\partial x}+\frac{\delta u_1-\delta u_3}{h_2}\right)\right.$$

$$\left.+I_2\left(\frac{d}{h_2}\frac{\partial\ddot{w}}{\partial y}+\frac{\ddot{v}_1-\ddot{v}_3}{h_2}\right)\left(\frac{d}{h_2}\frac{\partial\delta w}{\partial y}+\frac{\delta v_1-\delta v_3}{h_2}\right)\right]d\Omega+\int_\Omega q(x,y,t)\delta w d\Omega$$

$$-\int_\Omega\eta_2\left[\left(d\frac{\partial\dot{w}}{\partial x}+\dot{u}_1-\dot{u}_3\right)\left(\frac{d}{h_2}\frac{\partial\delta w}{\partial x}+\frac{\delta u_1-\delta u_3}{h_2}\right)+\left(d\frac{\partial\dot{w}}{\partial y}+\dot{v}_1-\dot{v}_3\right)\left(\frac{d}{h_2}\frac{\partial\delta w}{\partial y}+\frac{\delta v_1-\delta v_3}{h_2}\right)\right]d\Omega=0$$

(7)

where $\left(A_{jk}^{(i)},B_{jk}^{(i)},D_{jk}^{(i)}\right)=\int_{-h_i/2}^{h_i/2}(1,z_i,z_i{}^2)\bar{Q}_{jk}dz_i$ are the rigidity constants, in which the indices j and k can be 1, 2, or 6; and one should note that $B_{jk}^{(i)}{=}0$, when the panels are symmetrically laminated with respect to their mid-plane.   Next, performing the integration by parts with respect to the time variable in the Hamilton's principle (Eq. 5), and subsequent use of the classical gradient theorem, while taking advantage of the fundamental lemma of calculus of variations, after some tedious but standard manipulations (see [5]), one obtains the final form of the system displacement equations of motion and the associated boundary conditions.

2.3 SYSTEM DYNAMIC RESPONSE

At this point, the plate is assumed to be simply supported all around, so the displacement components u_i, v_i, and w, which identically satisfy the pertinent essential and natural boundary conditions, may advantageously be expanded as double Fourier series in the form [18]

$$u_i(x,y,t)=\sum_{n=1}^\infty\sum_{m=1}^\infty U_{mn}^{(i)}(t)\cos(\alpha_mx)\sin(\beta_ny),$$

$$v_i(x,y,t)=\sum_{n=1}^\infty\sum_{m=1}^\infty V_{mn}^{(i)}(t)\sin(\alpha_mx)\cos(\beta_ny),$$

(8)

$$w(x,y,t)=\sum_{n=1}^\infty\sum_{m=1}^\infty W_{mn}(t)\sin(\alpha_mx)\sin(\beta_ny),$$

where $U_{mn}^{(i)}(t)$, $V_{mn}^{(i)}(t)$ $(i{=}1,3)$, $W_{mn}(t)$ are unknown time dependent displacement coefficients, and $\alpha_m=m\pi/a$ and $\beta_n=n\pi/b$, and the above summations may be truncated to include $(n=1,2,...,N)\times(m=1,2,...,M)$ terms. Implementation of the above Fourier series solutions into the coupled set of partial differential equations of motion, and making use of the classical orthogonality relations for trigonometric functions, results in five

coupled ordinary differential equations in the time domain. Subsequent application of Laplace transform with respect to the time variable leads to five coupled algebraic equations in the s-domain, which for symmetrically laminated panels (i.e., for $B_{jk}^{(i)}=0$), can advantageously be put in the matrix form :

$$\mathbf{Z}_{mn}(s)\,\boldsymbol{\xi}_{mn}(s) = \mathbf{q}_{mn}(s)\,, \tag{9}$$

where

$$\boldsymbol{\xi}_{mn}(s) = \left[\tilde{U}_{mn}^{(1)}(s), \tilde{U}_{mn}^{(3)}(s), \tilde{V}_{mn}^{(1)}(s), \tilde{V}_{mn}^{(3)}(s), \widetilde{W}_{mn}(s)\right]^{T},$$
$$\mathbf{q}_{mn}(s) = [0, 0, 0, 0, \tilde{q}_{mn}(s)]^{T},$$

in which $\tilde{q}_{mn}(s) = \int_0^a \int_0^b \tilde{q}(x, y, s) \sin(\alpha_m x) \sin(\beta_n y) dy dx$ and "tilde" denotes Laplace transformation with respect to the time variable.

Now, it is difficult to find the analytical inverse Laplace transform of the complicated solution of matrix Eq. 9 for the transverse transformed displacement coefficients, $\widetilde{W}_{mn}(s)$. So, one has to resort to numerical computations. Accordingly, the complex inversion formula for Laplace transform is written as [19]

$$W_{mn}(t) = \frac{1}{2\pi i}\int_{\chi-j\infty}^{\chi+j\infty} \widetilde{W}_{mn}(s)e^{st}ds\,, \tag{10}$$

where $j = \sqrt{-1}$, and χ is an arbitrary real number greater than all the real parts of the singularities of $\widetilde{W}_{mn}(s)$. To obtain the dynamic response solution in the current work, Durbin's approach [20] for inversion of the Laplace transforms which involves the *discretized* form of the complex Laplace inversion formula (Eq. 10) in the interval $[0, 2T_0]$ shall be adopted. Thus, one could readily employ the expansion [21]

$$W_{mn}(t) = \frac{2e^{\chi t}}{T_0}\left[\frac{1}{2}\text{Re}\{\widetilde{W}_{mn}(\chi)\} + \sum_{l=1}^{\bar{N}}\left[\text{Re}\left\{\widetilde{W}_{mn}\left(\chi + j\frac{2\pi l}{T_0}\right)\right\}\cos\left(\frac{2\pi l}{T_0}t\right) - \text{Im}\left\{\widetilde{W}_{mn}\left(\chi + j\frac{2\pi l}{T_0}\right)\right\}\sin\left(\frac{2\pi l}{T_0}t\right)\right]\right]\,,$$
$$\tag{11}$$

where $\bar{N}$ is the truncation constant and the suggested value of "χT_0" is between 5 and 10 for sufficient accuracy [20].

2.4 SLIDING MODE CONTROL DESIGN

Sliding mode or variable structure control (SMC or VSC) strategy is one of the inherently robust control methods which have many good features such as insensitivity to system parameter variations, external disturbance rejection and good transient performance ([22], [23]). In the theory of sliding model control (SMC), a rapid switching (discontinuous) control action is generally used to switch between two values or gains with the objective of bringing the system's state space trajectory onto a specified hyper surface called the "switching manifold," which determines the closed loop system behavior [24]. The SMC design procedure can commonly be divided into two stages: sliding surface design where the system is restricted to remain on a linear hyper-plane in the state space, and control synthesis which will drive the system's state space trajectory onto to the designed surface by switching rapidly between two values or gains. In both stages, the system states are necessary to complete the implementation. Once the system reaches to the sliding surface, its behavior is characterized by the hyper-plane. Also, the infinitely fast switching control

can produce an undesirable chatter motion, which may be overcome by using a continuous approximation to SMC by using a sliding sector instead of a single switching plane/line [25]. Consequently, a good approximation to the ideal sliding motion is obtained and the basic SMC system design procedures and associated properties are retained. In what follows, the general sliding mode control strategy used for dynamic response control of the rectangular ERF-based sandwich plate is briefly outlined.

By adopting the so-named Kerwin's weak core assumption, which requires the net longitudinal forces in the ERF-based sandwich plate to vanish (i.e., $E_1 h_1 u_1 = E_3 h_3 u_3$ and $E_1 h_1 v_1 = E_3 h_3 v_3$; [26]), the dynamic equations of motion (A-1), may advantageously be casted in the state-space form as:

$$\dot{\mathbf{x}}(t) = \mathbf{f}(\mathbf{x}) + \mathbf{g}(\mathbf{x})\mathbf{u}(t) + \mathbf{\Gamma}\, \mathbf{d}(t), \tag{12}$$

where the $(6MN \times 1)$ state vector, $\mathbf{x}(t) = [\mathbf{U}(t); \mathbf{V}(t); \mathbf{W}(t); \dot{\mathbf{U}}(t); \dot{\mathbf{V}}(t); \dot{\mathbf{W}}(t)]^{\mathrm{T}}$, may explicitly be defined as

$$\mathbf{x}(t) = \Big[U_{11}^{(1)}, U_{12}^{(1)}, \dots, U_{1N}^{(1)}, U_{21}^{(1)}, \dots, U_{MN}^{(1)}; V_{11}^{(1)}, V_{12}^{(1)}, \dots, V_{1N}^{(1)}, V_{21}^{(1)}, \dots, V_{MN}^{(1)};$$
$$W_{11}, W_{12}, \dots, W_{1N}, W_{21}, \dots, W_{MN}; \dot{U}_{11}^{(1)}, \dot{U}_{12}^{(1)}, \dots, \dot{U}_{1N}^{(1)}, \dot{U}_{21}^{(1)}, \dots, \dot{U}_{MN}^{(1)};$$
$$\dot{V}_{11}^{(1)}, \dot{V}_{12}^{(1)}, \dots, \dot{V}_{1N}^{(1)}, \dot{V}_{21}^{(1)}, \dots, \dot{V}_{MN}^{(1)}; \dot{W}_{11}, \dot{W}_{12}, \dots, \dot{W}_{1N}, \dot{W}_{21}, \dots, \dot{W}_{MN} \Big]^{T}$$

$\mathbf{u}(t) = [E(t)]$ is the (1×1) control input (i.e., the time dependant electric field), $\mathbf{d}(t) = [\mathbf{0}; \mathbf{0}; q_{11}, q_{12}, \dots, q_{1N}, q_{21} \dots, q_{MN}; \mathbf{0}; \mathbf{0}; \mathbf{0}]^{\mathrm{T}}$ is the external disturbance (excitation), in which $q_{mn}(t) = \int_0^a \int_0^b q(x,y,t) \sin(\alpha_m x) \sin(\beta_n y) dy dx$, and the disturbance coefficient matrix, $\mathbf{\Gamma}$, along with the so-called smooth vector fields $\mathbf{f}$ and $\mathbf{g}$, are given as

$$\mathbf{\Gamma} = \mathbf{\Psi}^{-1}, \mathbf{f}(\mathbf{x}) = \mathbf{\Gamma}\, \mathbf{\Phi}\, \mathbf{x}(t),$$
$$\mathbf{g}(\mathbf{x}) = \mathbf{\Gamma}\, \mathbf{\Theta}\, \mathbf{x}(t) + \mathbf{\Gamma}\, \mathbf{\Upsilon}\, \bar{\mathbf{x}}(t),$$

where $\bar{\mathbf{x}}(t) = [\dot{\mathbf{U}}(t); \dot{\mathbf{V}}(t); \dot{\mathbf{W}}(t); \mathbf{0}; \mathbf{0}; \mathbf{0}]^{\mathrm{T}}$ is a subset of the state vector $\mathbf{x}(t)$, with $3MN$ nonzero elements, which is defined as

$$\bar{\mathbf{x}}(t) = \Big[\dot{U}_{11}^{(1)}, \dot{U}_{12}^{(1)}, \dots, \dot{U}_{1N}^{(1)}, \dot{U}_{21}^{(1)}, \dots, \dot{U}_{MN}^{(1)}; \dot{V}_{11}^{(1)}, \dot{V}_{12}^{(1)}, \dots, \dot{V}_{1N}^{(1)}, \dot{V}_{21}^{(1)}, \dots, \dot{V}_{MN}^{(1)};$$
$$\dot{W}_{11}, \dot{W}_{12}, \dots, \dot{W}_{1N}, \dot{W}_{21}, \dots, \dot{W}_{MN}; 0,0, \dots,0; 0,0, \dots,0; 0,0, \dots,0 \Big]^{T}$$

As the first step in the sliding mode control (SMC) scheme, the sliding surface $\sigma(t)$ is defined as

$$\sigma(t) = \mathbf{S}\, \mathbf{x}(t), \tag{13}$$

where $\mathbf{S}(1 \times 6MN)$ is the so-called sliding surface matrix, which represents the slope of the sliding surface and may be represented as

$$\mathbf{S} = [\mathbf{0}; \mathbf{0}; S_{11}^{(1)}, S_{12}^{(1)}, \dots, S_{1\widetilde{N}}^{(1)}, 0, \dots,0, S_{21}^{(1)}, S_{22}^{(1)}, \dots, S_{2\widetilde{N}}^{(1)}, 0, \dots,0, \dots, S_{\widetilde{M}1}^{(1)}, S_{\widetilde{M}2}^{(1)}, \dots, S_{\widetilde{M}\widetilde{N}}^{(1)}, 0, \dots,0$$
$$;\mathbf{0}; \mathbf{0}; S_{11}^{(2)}, S_{12}^{(2)}, \dots, S_{1\widetilde{N}}^{(2)}, 0, \dots,0, S_{21}^{(2)}, S_{22}^{(2)}, \dots, S_{2\widetilde{N}}^{(2)}, 0, \dots,0, \dots, S_{\widetilde{M}1}^{(2)}, S_{\widetilde{M}2}^{(2)}, \dots, S_{\widetilde{M}\widetilde{N}}^{(2)}, 0, \dots,0]^{\mathrm{T}}$$

where there are a total of $2\widetilde{M}\widetilde{N}$ nonzero elements, and $\widetilde{M}\widetilde{N}$ is the total number of controlled modes. This matrix is selected such that a stable motion for the closed loop system occurs. Also, in the controller design stage, the control input is designed such that the system trajectories reach the sliding surface in a finite time (reaching phase) and then stays on the sliding surface (sliding phase). The existence condition of the sliding mode motion is given by ([27], [25]):

$$\frac{1}{2}\frac{d}{dt}\sigma^2(t) \le -\eta \, |\sigma(t)|, \tag{14}$$

where η is a strictly positive constant. The above condition allows the state variable $\mathbf{x}(t)$ to converge to the sliding surface $\sigma(t)$.

Devising a control strategy which satisfies the existence condition of the sliding mode motion (14), while it avoids the chattering problem, can be accomplished by implementation of a smoothed control strategy in the form ([27], [25])

$$u(t) = -[\mathbf{S}\,\mathbf{g}(\mathbf{x})]^{-1}\{\mathbf{S}\,\mathbf{f}(\mathbf{x}) + (k - \dot{\Xi})\mathrm{sat}[\sigma(t)/\Xi(t)]\}, \tag{15}$$

where the discontinuous control gain, k, should satisfy the condition $k > |\mathbf{S}\,\boldsymbol{\Gamma}\,f_{ub}| + \eta$, in which f_{ub} is the upper bound of the excitation force $\mathbf{d}(t)$. Also, the saturation function, sat $(.)$, which is continuous inside the boundary layer thickness, $\Xi(t)$, is given by

$$\mathrm{sat}\big(\sigma(t)/\Xi(t)\big) = \begin{cases} \sigma(t)/\Xi(t), & |\sigma(t)| \le \Xi(t), \\ \mathrm{sgn}\big(\sigma(t)/\Xi(t)\big), & |\sigma(t)| > \Xi(t), \end{cases} \tag{16}$$

where sgn$(.)$ is the classical sign function, $\Xi(t)$ satisfies $\dot{\Xi}(t) = -\kappa\,\Xi(t) + k$, $\Xi(0) = \eta/\kappa$, and κ (a strictly positive constant) is the break-frequency (bandwidth) of a first order low pass filter. In order to eliminate the chattering problem, the value of κ must be chosen to be "small" with respect to high-frequency unmodelled dynamics of the system so that these structural modes are not excited.

Lastly, it should be noted that the control inputs of a dynamic system are usually restricted by its physical parameters. This means that the system inputs have generally the character of saturation. Accordingly, the continuous controllers (15) may be constrained within the range [28]:

$$u(t) = \begin{cases} u(t), & |u(t)| \le u_{\max}, \\ u_{\max}\mathrm{sgn}\big(u(t)\big), & |u(t)| > u_{\max}, \end{cases} \tag{17}$$

where $u_{\max}$ is the upper bound of $u(t)$ (i.e., the maximum permitted control input with a positive value), which is specified in terms of the physical devices used in practical applications. The controller presented in Eq. 17 is referred to as the saturated controllers, since the control effort $u(t)$ is saturated at $u_{\max}$. This completes the necessary background required for the analysis of the problem. Next we consider some numerical examples.

3 NUMERICAL RESULTS

In order to illustrate the nature and general behavior of the solution, we consider some numerical examples in this section. Realizing the large number of parameters involved here while keeping in view our computing hardware limitations, we confine our attention to a particular model. Square sandwich isotropic aluminum/ERF/aluminum plates of selected geometric parameters $\big(a = b = 0.5\mathrm{m};\ h_{1,3} = 0.0005\mathrm{m};\ h_2 = 0.002\mathrm{m}\big)$ are considered. The material parameters for the aluminum layers are given as $\rho_{1,3} = 2700\mathrm{kg/m^3}$; $E_{1,3} = 70\mathrm{GPa}$; $v_{1,3} = 0.3$. Based on the existing information on the ER material pre-yield rheology, only the electric field dependence of ER material in the pre-yield regime is to be considered. In this regime, input parameters corresponding to our first order isotropic Kelvin-Voigt viscoelastic model (see Eq. 4) used for the electrorheological core fluid layer subject to the time-dependant electric field ($0 \le E(t) \le 5\mathrm{kV/mm}$) is as follows: $m_e = 0.27, b_e = 3.73$, $m_g = 1500, b_g = 0$ [17], with $\rho_2 = 1700\mathrm{kg/m^3}$ being the mass density of the ER fluid. A

Mathematica code was constructed for treating the linear system (9), solving for the unknown transformed displacement coefficient $\widetilde{W}_{mn}(s)$, and ultimately calculating the transverse displacement response $w(x, y, t)$ using Durbin's Laplace inversion algorithm (11) for a given electric field magnitude and selected geometric parameters and external loading specifications. Three distinct loading configurations with zero initial conditions are considered. Also, the adaptive plate may rest on either of the following isotropic Winkler-Pasternak elastic foundations:

Soft Foundation: $G_f = 10^2 \text{N/m}, K_f = 10^3 \text{ N/m}^3$,
Stiff Foundation: $G_f = 10^4 \text{N/m}, K_f = 10^5 \text{ N/m}^3$.

The convergence of results was systematically checked in a simple trial and error manner, by increasing the truncation constants $(N, M, \overline{N})$ while looking for steadiness or stability in the numerical value of the solutions. Using a maximum number of nine modes ($N_{max} = M_{max} = 3$), and a truncation constant of $\overline{N}_{max} = 1000$ ($\chi T_0 = 4.5$) were found to yield satisfactory results for the selected geometric parameters in all loading situations. Also, for active control of the dynamic response, the smoothed sliding mode control strategy (15) was implemented into the state space form of the dynamic system equations (12), with a maximum number of nine structural/controlled modes ($N_{max} = M_{max} = \widetilde{N}_{max} = \widetilde{M}_{max}=3$), and subsequent application of the 4th order Runge-Kutta time integration algorithm with a minimum step size of $\Delta t = 10^{-5}$(sec). Lastly, an upper bound of $u_{max} = 5$(kV/mm) was set as the saturation electric field in the controller law (17), and the key controller parameters are selected as $(\eta = 0.1, k = 1, \kappa = 100)$.

Figure 2 shows the time-variation of the transverse center-point plate displacement response, $w(x = a/2, y = b/2; t)$ (meter), with or without the soft/stiff foundation interaction, for the selected loading configurations and selected electric field strengths ($E = 0.5$kV/mm). Also shown, is the closed-loop response of the system under sliding-mode control.
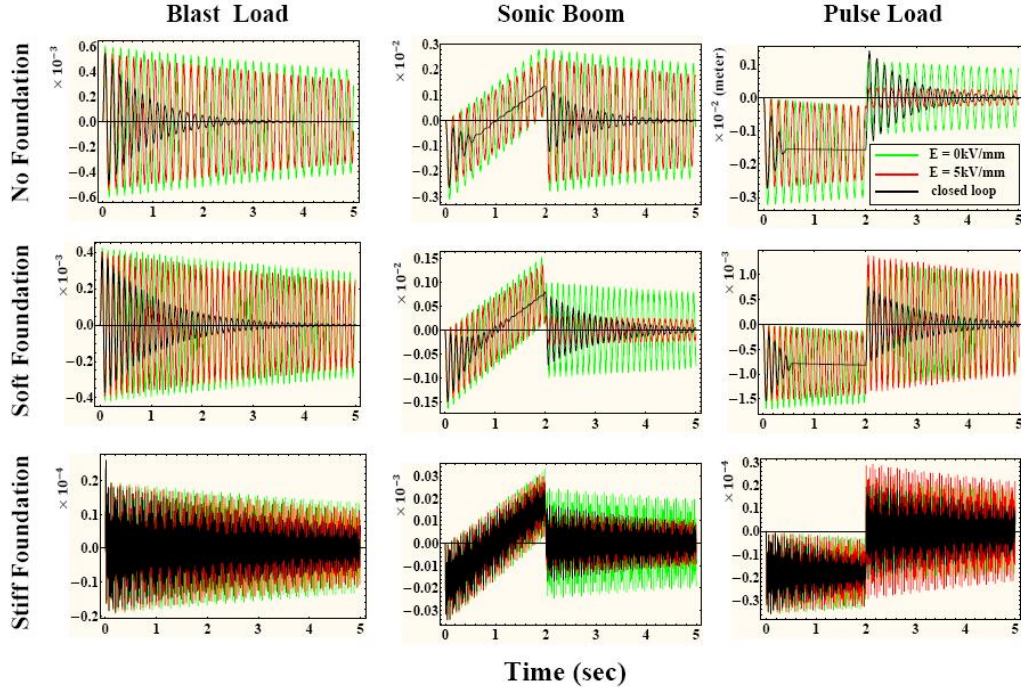

Figure 2: Dynamic response of the plate under different loadings

The first column in Fig. 3 displays the center-point plate displacement response due to an impulsive central point load, with or without the soft/stiff foundation coupling, for two different truncation constants ($N = M = 2,3$), and selected electric field strength ($E = 5$ kV/mm). It is clear that as the foundation stiffness decreases, the convergence of results becomes slightly easier. Also, the acceptable convergence of numerical results with inclusion of a total of four structural modes ($N = M = 2$) is apparent from the figure. The second column in Fig. 3 displays the closed-loop center-point response of the system under the sliding-mode control law for the impulsive central point load, with or without the soft/stiff foundation coupling, for inclusion of a total of nine structural modes ($N = M = 3$), and with two different numbers of controlled modes ($\widetilde{N} = \widetilde{M} = 2,3$). The effectiveness of the control action in suppressing the panel vibration in addition to the close agreements of the stable time response curves indicate that when the higher order modes are included in the simulation, the structure is not excited by the spillover phenomena. In other words, since energy is always being dissipated, the sliding mode control strategy employed here is insensitive to the control spillover problems generally encountered in the fully-active control cases due to the excitation of residual modes ([29], [30]).
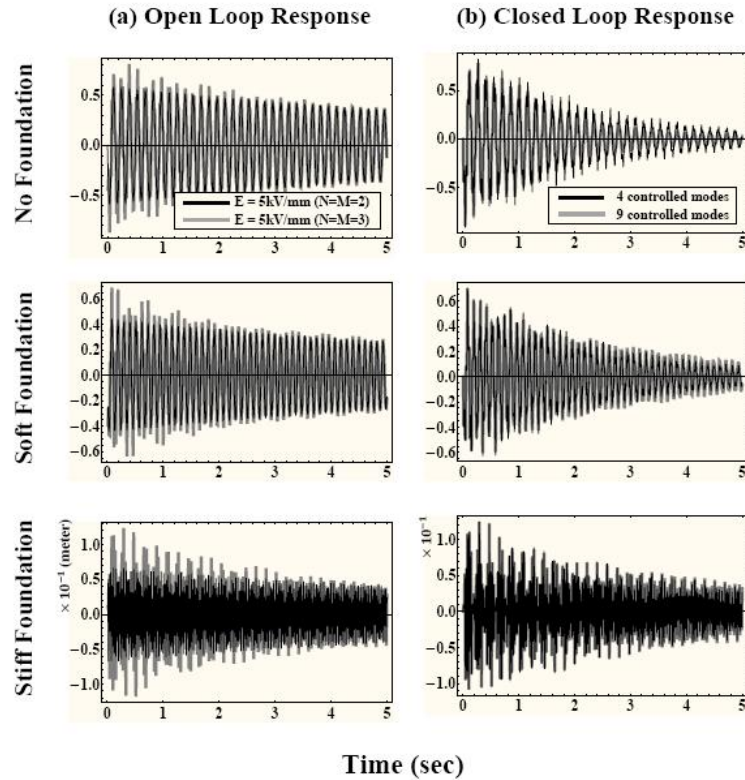

Figure 3: Dynamic responses of the plate with different numbers of considered modes

4 CONCLUSIONS

The performance, effectiveness, robustness, and insensitivity with respect to the spillover of the proposed SMC-based control system are demonstrated through comprehensive numerical simulations. In particular, in the absence of elastic foundation, or in case of the adaptive plate coupled to a weak foundation, the ERF-based sliding mode control strategy is found to be a very effective means of dynamic response suppression,

especially for purely transient loads (e.g., for the moving load, or the impulse load). On the other hand, when the structure is perfectly bonded to a stiff foundation and excited by a continuous time-domain load (e.g., a harmonic load), the vibration suppression performance of the ERF-layer is severely deteriorated and other control methods may be sought. Moreover, the effectiveness of the sliding mode strategy when the higher order control modes are excluded indicates that the structural performance is not degraded by the spillover phenomenon which is generally encountered in the fully-active control problems due to the excitation of residual modes. It is hoped that the present study will provide designers the basic information required in practical structural control applications involving ER fluid-based smart structures.

NOTE: Detailed derivations of the equations and matrices elements are available upon request.

REFERENCES

[1] I. Chopra, Review of state of art of smart structures and integrated systems. *AIAA Journal*, **40** (11), 2145–2187, 2002.

[2] S.V. Gopinathan, V.V. Varadan, V.K. Varadan, A review and critique of theories for piezoelectric laminates. *Smart Materials and Structures,* **9** (1), 24–48, 2000.

[3] B.S. Balapgol, S.A. Kulkarni, K.M. Bajoria, A review on shape memory alloy structures. *International Journal of Acoustics and Vibrations,* **9** (2), 61-68, 2004.

[4] F. Pablo, D. Osmont, R. Ohayon, Modeling of plate structures equipped with current driven electrostrictive actuators for active vibration control. *Journal of Intelligent Material Systems and Structures,* **14** (3), 173-183, 2003.

[5] S.M. Hasheminejad and M. Maleki, Free vibration and forced harmonic response of an electrorheological fluid-filled sandwich plate. *Smart Materials and Structures,* **18** (5), Art No. 055013, 2009.

[6] M. Yalcintas and H. Dai, Vibration suppression capabilities of magnetorheological materials based adaptive structures. *Smart Materials and Structures,* **13** (1), 1-11, 2004.

[7] Y.S. Kim, K.W. Wang, H.S. Lee, Feedback control of ER-fluid-based structures for vibration suppression. *Smart Materials and Structures,* **1**, 139–145, 1992.

[8] K.W. Wang, Y.S. Kim, D.B. Shea, Structural vibration control via electrorheological-fluid-based actuators with adaptive viscous and frictional damping. *Journal of Sound and Vibration,* **177** (2), 227–237, 1994.

[9] G. Leitmann and E. Reithmeier, Semiactive control of a vibrating system by means of electrorheological fluids. *Dynamics and Control,* **3**, 7–33, 1993.

[10] C.D. Rahn and S. Joshi, Modeling and control of an electrorheological sandwich beam. *Journal of Vibration and Acoustics,* **120**, 221-227, 1998.

[11] Y. Kuroda, T. Ura, S. Morishita, Adaptive neural-network vibration control with electrorheological dynamic damper. *Theoretical and Applied Mechanics,* **41**, 29–34, 1992.

[12] N.D. Sims, R. Stanway, S.B.M. Beck, Proportional feedback control of an electro-rheological vibration damper. *Journal of Intelligent Material Systems and Structures,* **8**, 426–433, 1997.

[13] M. Nakano, A novel semi-active control of automobile suspension using an electro-rheological shock absorber. *ER Fluids, MR Suspensions and Associated Technology*, 634-653, 1996.

[14] S.B. Choi and Y.K. Park, Active vibration control of cantilevered beam containing an electrorheological fluid. *Journal of Sound and Vibration,* **172**, 428–432, 1994.

[15] J.Y. Yeh, J.Y. Chen, C.T. Lin, C.Y. Liu, Damping and vibration analysis of polar orthotropic annular plates with ER treatment. *Journal of Sound and Vibration,* **325** (1-2), 1-13, 2009.

[16] J.N. Reddy, *Theory and Analysis of Elastic Plates and Shells (Second Edition).* CRC Press, USA, 2006.

[17] J.P. Coulter, T.G. Duclos, D.N. Acker, The usage of electrorheological materials in viscoelastic layer damping applications. *Proceedings of Damping, Palm Beach, Florida*, 1989.

[18] A.W. Leissa, *Vibration of Plates.* Columbus, Acoustical Society of America, 1993.

[19] F.B. Hildebrand, *Advanced Calculus for Applications.* Prentice-Hall, Englewood Cliffs, New Jersey, USA, 1976.

[20] F. Durbin, Numerical inversion of Laplace transforms: an effective improvement of Dubner and Abate's method. *The Computer Journal,* **17** (4), 371-376, 1973.

[21] S.M. Hasheminejad, S. Abbasion, A. Bahari, Time domain computation and visualization of shock induced sound fields for a doubly fluid-loaded hollow cylinder. *Computers and Structures,* **88**, 1077-1091, 2010.

[22] V.I. Utkin, *Sliding Modes and Their Application in Variable Structure Systems.* MIR Publishers, Moscow, 1974.

[23] C. Edwards, S.K. Spurgeon, *Sliding Mode Control: Theory and Applications.* Taylor & Francis, London, 1998.

[24] M. Allen, F. Bernelli-Zazzera, R. Scattolini, Sliding mode control of a large flexible space structure. *Control Engineering Practice,* **8** (8), 861–871, 2000.

[25] W. Perruquetti, J.P. Richard, P. Borne, A generalized regular form for multivariable sliding mode control. *Mathematical Problems in Engineering,* **7**, 15-27, 2001.

[26] D.J. Mead and S. Markus, The forced vibration of a three-layer, damped sandwich beam with arbitrary boundary conditions. *Journal of Sound and Vibration,* **10** (2), 163-175, 1969.

[27] J.J.E. Slotine, L. Weiping, *Applied Nonlinear Control.* Prentice Hall, Englewood Cliffs, New Jersey, 1991.

[28] Y. Chao, S. Chen, W. ZhiGang, X. ChangChuan, Application of output feedback sliding mode control to active flutter suppression of two-dimensional airfoil. *Science China Technological Sciences,* **53**, 1338-1348, 2010.

[29] Y.A. Khulief, Vibration suppression in rotating beams using active modal control. *Journal of Sound and Vibration,* **242** (4), 681-699, 2001.

[30] M.J. Balas, Trends in large space structure control theory: fondest hopes, wildest dreams. *IEEE Transactions on Automatic Control,* **AC-27** (3), 522-535, 1982.